

# Nano-Engineered Erythrocyte Ghosts as Inhalational Carriers for Delivery of Fasudil: Preparation and Characterization

Nilesh Gupta · Brijeshkumar Patel · Fakhru Ahsan

Received: 24 September 2013 / Accepted: 5 December 2013 / Published online: 22 January 2014  
© Springer Science+Business Media New York 2014

## ABSTRACT

**Purpose** Nanoerythrocytes (NERs), an engineered derivative of erythrocytes, have long been used as drug delivery carriers. These cell based carriers are biocompatible and biodegradable, and they exhibit efficient drug loading, targeting specificity and prolonged biological half-life. In this study, we have evaluated the feasibility of NERs as inhalable carriers for delivery of fasudil, an investigational drug for the treatment of pulmonary arterial hypertension.

**Methods** We prepared NERs by hypotonic lysis of erythrocytes derived from rat blood followed by extrusion through polycarbonate membranes. The formulations were optimized and characterized for size, morphology, entrapment efficiency, stability, cellular uptake and *in-vitro* release profiles followed by monitoring of drug absorption and safety evaluation after intratracheal administration of fasudil-loaded NERs into rats.

**Results** NERs were spherical in shape with an average size of  $154.1 \pm 1.31$  nm and the drug loading efficiency was  $48.76 \pm 2.18\%$ . Formulations were stable when stored at  $4^{\circ}\text{C}$  for 3 weeks. When incubated with rat pulmonary arterial smooth muscle cells (PASM), a significant amount of NERs was taken up by PASM cells. The drug encapsulated in NERs inhibited the rho-kinase activity upto 50%, which was comparable with the plain fasudil. A ~6–8 fold increase in the half-life of fasudil was observed when encapsulated in NERs.

**Conclusion** This study suggests that nanoerythrocytes can be used as cell derived carriers for inhalational delivery of fasudil.

**KEY WORDS** fasudil · nanoerythrocytes · pulmonary arterial hypertension · pulmonary delivery

## ABBREVIATIONS

ALP	Alkaline phosphatase
BALF	Bronchoalveolar lavage fluid
EGM	Endothelial growth medium
FBS	Fetal bovine serum
FITC	Fluorescein isothiocyanate
HBSS	Hanks balanced salt solution
HRP	Horseradish peroxidase
IV	Intravenous
IT	Intratracheal
LDH	Lactate dehydrogenase
LPA	Lysophosphatidic acid
NERs	Nanoerythrocytes
PAE	Pulmonary arterial endothelial
PAH	Pulmonary arterial hypertension
PASMC	Pulmonary arterial smooth muscle cells
PBS	Phosphate buffered saline
ROCK	Rho-kinase
rMYPT-1	Recombinant myosin phosphatase target subunit-1
SD	Sprague Dawley
TMB	Tetramethylbenzidine

## INTRODUCTION

Nanoparticles adopted various names such as functionalized, targeted, magnetic, hybrid, stealth and biomimetics depending on the material and surface property of the particles (1,2). Stem cells, bacterial ghosts and viral particles have been used as biomimetic carriers for delivery of both small and large molecular weight therapeutic agents (3,4). Of the blood cell based biomimetic carriers, nanoerythrocytes (NERs), nanosized capsules derived from erythrocytes, exhibit many favorable properties with regard to biodegradation, release profiles and targeting efficiency (5,6). NERs have a very high surface area-to-volume ratio (~ 80 times higher than parent

N. Gupta · B. Patel · F. Ahsan (✉)  
Department of Pharmaceutical Sciences, School of Pharmacy  
Texas Tech University Health Sciences Center, 1300 Coulter Drive  
Amarillo, Texas 79106, USA  
e-mail: fakhru.ahsan@ttuhsc.edu

erythrocyte) that contributes to their prolonged circulation time in the blood. NERs could be as small as 100 nm and can move around the body with high drug payload (7).

However, preparation of NERs demands extra care for handling of erythrocytes and requires a correct combination of internal and external medium for maximal drug loading (8,9). To load therapeutic agents into erythrocytes, hemoglobin and cytoplasmic content of the cells must be removed using hypotonic solution mediated lysis (hemolysis). But the process of removal of intracellular contents must be performed in a controlled manner. The removal process should not disrupt cells' plasma membrane but allow cells to form seamless nanosized capsules. Depending on the percent cell recovered after stripping the cell off its organelles, one erythrocyte can be fragmented into 4000–5000 NERs. Sonication, extrusion and electric pulses have been used to prepare NERs from hemoglobin free erythrocyte ghosts. Of these sizing methods, extrusion is the most efficient technique to achieve uniform NERs with minimal cell loss. Moreover, the flexibility and fluidity of NERs play important roles in the stability and the shelf-life of the formulations. Thus, an optimal combination of lysis media, processing temperature and sizing technique is required to develop a stable and viable NERs based formulation (10,11).

Because of the biomimetic property, NERs have been used for encapsulation of enzymes, peptides, toxins, genetic materials and contrast agents (6,12). Many investigators have evaluated the feasibility of NERs as drug carriers for the treatment of disorders related to the liver, spleen, lymph nodes and different types of cancers (13–15). Daunorubicin and pyrimethamine, for example, were conjugated onto nanoerythroosomal surfaces (15,16). But to our knowledge, no small molecular weight drugs have directly—without conjugation—been encapsulated into NERs. Further, use of NERs as drug carriers has been limited to intravenous, intraperitoneal and subcutaneous routes of administration. They are yet to be investigated as inhalational drug carriers.

Fasudil, an investigational drug, has been used in the inhalation therapy for pulmonary arterial hypertension (PAH). This is a disorder of cardio-respiratory system that results in elevated pulmonary arterial pressure, vascular remodeling and subsequent right ventricular failure (17). But fasudil has a very short half-life that can be extended by encapsulating in liposomes. Recently, we have shown that liposomal fasudil produce a sustained pulmonary vasodilation after intratracheal administration (18). Others have also documented that fasudil, a highly soluble drug with a  $pK_a$  of 9.72, can be encapsulated in liposomes by pH gradient based remote loading. Since NERs are cell based capsules with semi-permeable membrane, we assume that fasudil could be efficiently encapsulated into NERs without any pH gradient. However, we do not know the optimal conditions for maximal encapsulation of the drug in NERs. The stability, loading

efficiency, and pharmacokinetic and safety profiles of NERs containing fasudil are also unknown. In the present study, we have evaluated the feasibility of NERs as carriers for the inhalational delivery of a small molecular weight drug, fasudil, a specific Rho-kinase (ROCK) inhibitor that works as a potent vasodilator. In contrast to the previously published studies that conjugated large/small molecular weight drugs on NERs surface, we have optimized the processing parameters to load drug directly into the NERs. We have tested the entrapment efficiency, controlled release behavior, storage stability, *in-vivo* absorption profiles and safety for administration into the lungs.

## MATERIALS AND METHODS

### Materials

Fasudil monohydrochloride was purchased from LC labs, Inc. (Woburn, MA, USA). Sephadex-G-25 PD-10 pre-packed columns and Ficoll-Paque PLUS were from GE Healthcare Biosciences (Piscataway, NJ, USA). All other chemicals including methanol, phosphate buffered saline (PBS 1X), acetonitrile, and dimethyl sulfoxide were of analytical grade and obtained from various vendors in the United States. All chemicals were used without further purification.

### Preparation of Erythrocyte Ghosts

To prepare erythrocyte ghosts, intracellular contents were first removed from the red blood cells collected from male Sprague–Dawley (SD) rats (175–225 g, Charles River Laboratories, Charlotte, NC) (Fig. 1) as reported previously (16,19). Briefly, blood was collected in a 50 ml tube containing sodium citrate via the inferior vena cava of the rats. Erythrocytes were separated from the blood by density centrifugation using Ficoll-Paque gradient. For separation, blood samples diluted with PBS (1X, pH 7.4) were added slowly into a centrifugation tube containing the Ficoll-Paque layer. The blood-Ficoll mixture was centrifuged at 500 g for 40 min at 18°C and then the serum and buffy coat were carefully removed. The resulting erythrocytes pellets were washed three times in PBS and stored at 4°C until further use. Erythrocytes were hemolysed by incubating them sequentially in 50 and 30 mOsm hypotonic solutions, prepared from isotonic PBS solution (~300 mOsm). The hemoglobin in the supernatant was removed after centrifugation and cream-colored pellet was resuspended in hypotonic solutions and subjected to centrifugation again. The colorless ghosts thus obtained were incubated in hypertonic solution (10X PBS) for 60 min at 37°C for resealing. The resulting sealed ghosts were washed 3 times with isotonic PBS and stored at 4°C until further use. The process of preparation of erythroosomes from erythrocytes was visualized under a fluorescence microscope (IX-81,

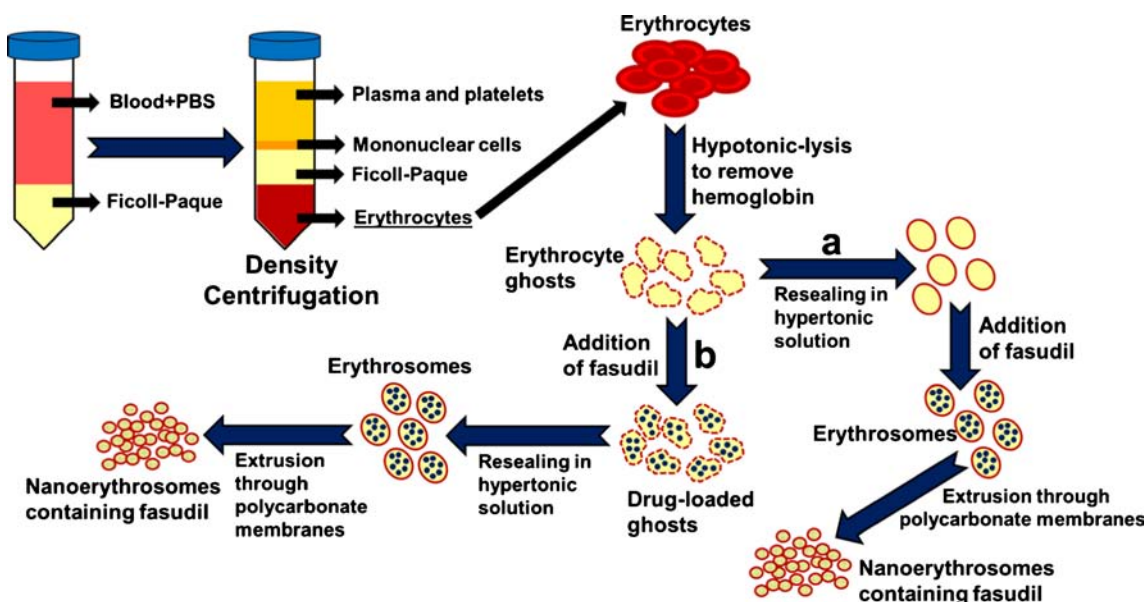


**Fig. 1** Schematic representation for preparation of nanoerythroosomes from rat whole blood by hypotonic lysis–extrusion method. Ficoll-Paque was used to separate erythrocytes from the blood. Hypotonic solution was prepared from PBS (1X, pH 7.4) by dilution. PBS 10X was used as the hypertonic solution for resealing.

Olympus, Center Valley, PA) at each stage by fixing the cells in formaldehyde solution (Fig. 2). Further, before loading the drug, we encapsulated fluorescein isothiocyanate-dextran (FITC-Dextran, 70 kDa, Sigma-Aldrich, St. Louis, MO) into the ghosts. To confirm resealing and loading, FITC-loaded erythrocytes were observed under the fluorescent microscope.

**Drug Loading**

Fasudil was loaded into the erythrocyte ghosts before (Fig. 1b, cells with pores) and after (Fig. 1a, resealed erythrocyte ghosts) closing the cell membrane pores. For drug loading into resealed ghosts, we first closed cell membrane pores by incubating the cells in hypertonic solution (10X PBS) for 60 min at 37°C. Then drug solutions containing varying concentrations

of fasudil (5–30 mg/ml) were incubated with an aliquot of sealed cells (Fig. 1). For loading drug before resealing, drug solution was incubated with the cells recovered from the hypotonic solution (Fig. 1). The drug loading was assessed by lysing the drug loaded ghosts (20 µl) with methanol (980 µl). The drug was finally separated from cellular carriers by sonication and centrifugation. The amount of fasudil in supernatant was measured at 320 nm using a UV spectrophotometer (UV/Vis 918, GBC Scientific Equipment, Hampshire, IL) and the percent drug loading was calculated using the following equation:  $Percent\ drug\ loading = (Amount\ of\ drug\ loaded / Amount\ of\ drug\ added) \times 100$ . We have also studied the influence of temperature on drug loading by incubating the drug solution with erythrocyte ghosts at three different temperatures (4°, 25° and 37°C) and subsequently quantitating the drug content.

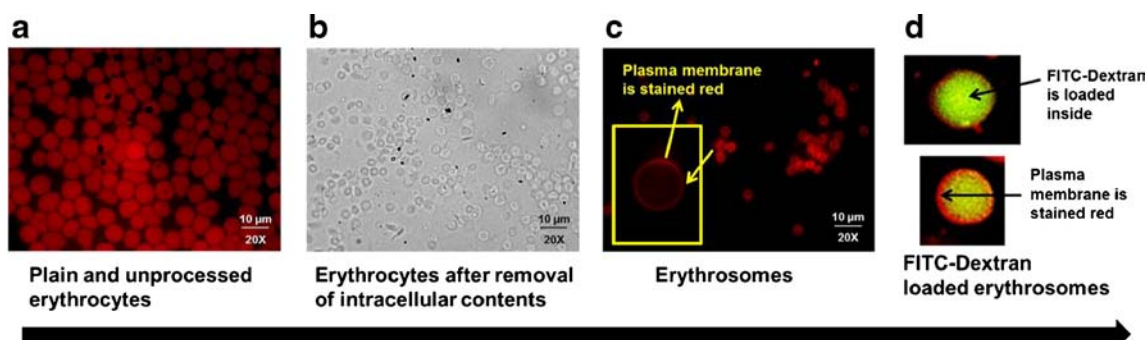


**Fig. 2** Fluorescent microscopic images of erythroosomes prepared from erythrocytes: plain and unprocessed erythrocytes (a), erythrocyte ghosts after removal of intracellular contents (b), erythroosomes stained with plasma membrane dye (c), and FITC-Dextran loaded erythroosomes (d) stained with plasma membrane dye (green color denotes FITC-Dextran and red color is for plasma membrane dye).

## Preparation of Nanoerythroosomes from Erythrocyte Ghosts Containing Fasudil

Nanoerythroosomes were prepared by reducing the size of erythrocyte ghosts containing fasudil. Three size reduction methods were used to prepare nanosized erythroosomes: (i) bath sonication (Bransonic 3510, Branson Ultrasonics Corporation, Danbury, CT), (ii) probe sonication (Branson Digital Sonifier 450, Branson Ultrasonics Corporation, Danbury, CT), and (iii) extrusion (LiposoFast® Extruder, Avestin, Inc., Canada). Sonication was performed for 15 min at 25°C and the drug was analyzed as indicated above. For extrusion, ghosts containing the drug were sequentially passed through polycarbonate membranes of different pore sizes (1.0, 0.8, 0.4 and 0.2 µm) and nanosized erythroosomes were collected after 21 cycles and stored at 4°C. Extrusion method used to reduce the size of erythrocyte ghosts was modified based on a published procedure (16). Un-encapsulated drug was removed by passing fasudil loaded NERs through a Sephadex-G-25 PD-10 column equilibrated with PBS (1X, pH 7.4).

The size and polydispersity of the optimized NERs containing fasudil were determined using a Malvern Zetasizer (Malvern® Instruments Limited, Worcestershire, UK). The morphology of the nanoerythroosomal formulations was evaluated using the fluorescence microscope.

## Evaluation of Stability Profiles

To evaluate the stability of fasudil-loaded NERs, an aliquot of the particles (500 µl) were stored at 4°C, 25°C and 37°C for 21 days. Samples were withdrawn each day (0, 7, 14 and 21) for determination of vesicle size and drug content as described above. The stability upon nebulization was determined with a PennCentury® Microsprayer (Model IA-1B, PennCentury, PA). Fasudil loaded NERs suspended in PBS were placed in the syringe attached with the aerosolizer and then sprayed ten times. The fine droplets thus generated were collected in a small tube for assessing vesicle size, polydispersity index and entrapment efficiency.

The centrifugal stability was assessed to determine the effect of centrifugation speeds on drug leakage from NERs. NERs containing fasudil (500 µl) were centrifuged at various speeds ranging from 1000 to 15000 rpm for 20 min at 4°C and the amount of drug released in supernatant was quantitated.

The drug leakage that may occur due to turbulence during handling and administration to animals was also evaluated. NERs containing fasudil were passed through a 27<sup>1/2</sup> gauge needle at a flow rate of 10 ml/min, comparable with the blood flow rate *in-vivo*. The number of passes was varied (5–20 times) in order to change the intensity of turbulence that may result due to repeated injections. The formulations were then centrifuged for quantitation of fasudil as described above.

The propensity of NERs to hemolyze blood was studied by incubating NERs with the whole blood and subsequently measuring the degree of hemolysis. NERs containing fasudil were added to whole blood at either 1:1 or 2:1 ratio and incubated at 37°C for 30 min in the dark followed by centrifugation for 10 min at 5000 rpm. The amount of hemoglobin released was determined in the supernatant by measuring the absorbance at 540 nm using a UV/visible spectrophotometer. A completely lysed blood sample (prepared by adding distilled water to whole blood) was used as a control. The percent hemoglobin release was calculated using the following equation:  $Percent\ hemolysed = ((A_{540\ of\ sample} - A_{540\ of\ background}) / (A_{540\ of\ 100\% \ Hemoglobin})) \times 100$ ;  $A_{540}$  is the absorbance at 540 nm.

## In Vitro Release Studies

The release profiles of drug from NERs containing fasudil were evaluated using dialysis cassettes (Slide-A-Lyzer, 3500 MWCO, 0.1–0.5 ml, Thermo-Scientific, Waltham, MA) as reported previously (18). Briefly, the cassettes were first hydrated for 30–60 min with PBS (pH 7.4) and NERs (500 µl) were loaded carefully using a syringe without puncturing the dialysis membrane. To assess whether dialysis cassettes serve as barriers to drug release, we used plain fasudil as control in this set of experiment. Cassettes were then immersed in a beaker containing 100 ml PBS and placed inside an incubator with preset temperature (37°C) along with moderate stirring. At predetermined time intervals, samples were withdrawn from the beaker and the media was immediately replenished with an equal volume of fresh PBS. The amount of drug released was estimated by a UV spectrophotometer as described above.

## Cellular Uptake of NERs

Three different cell lines—rat pulmonary arterial smooth muscle (PASM) cells, human pulmonary arterial endothelial (PAE) cells and rat alveolar macrophages—were used to study the cellular uptake of NERs (18,20). Rat PASM cells were cultured in 75 cm<sup>2</sup> corning flask using DMEM F-12 medium containing 10% fetal bovine serum (FBS), 1% penicillin/streptomycin and 1% 200 mM glutamine (ATCC, Manassas, VA) in a humidified incubator maintained at 37°C with 5% CO<sub>2</sub>. Human PAE cells were grown at the same condition using endothelial cell growth media (EGM-2 BulletKit, Lonza Inc., Allendale, NJ). After reaching ~90% confluency, rat PASM (P-7) and human PAE (P-2) cells were seeded at a density of 5 × 10<sup>3</sup> cells/ml and left in the humidified incubator for overnight attachment. Next day, NERs, stained with plasma membrane dye (CellMask™, Molecular Probes Inc., Eugene, OR), were incubated with cells for 2 h at 37°C. Following incubation, cells were fixed with a cold

mixture of acetone and methanol (1:1) and incubated with a blocking solution containing goat serum and Tween 20 in PBS. After this, cells were incubated with monoclonal anti- $\beta$ -actin primary antibodies (Sigma-Aldrich, St. Louis, MO) and Alexa Fluor® 495 goat anti-mouse IgG (Invitrogen, Grand Island, NY) sequentially. Glass coverslips were placed onto glass slides and uptake of the NERs was observed under a fluorescence microscope.

*Uptake of NERs by macrophages* was evaluated by incubating NERs containing FITC-Dextran with rat alveolar macrophages. Briefly, the lungs were surgically removed from anesthetized male SD rats (200–250 g) and bronchoalveolar lavage fluid (BALF) was collected by repeated washing of the lungs with  $\text{Ca}^{2+}$  and  $\text{Mg}^{2+}$  free Dulbecco's PBS containing 0.5 mM disodium EDTA as described in our previously published article (20). The resulting BALF containing macrophages was centrifuged to obtain the cell pellet, which was further suspended in Hank's Balanced Salt Solution (HBSS). The macrophages at a density of  $4 \times 10^5$  cells/ml were seeded onto coverslips placed in a 12-well plate and incubated in a humidified chamber at 37°C for 1 h. Attachment of macrophages onto coverslips was examined under a bright-field microscope (VanGuard 1200 CME, VEE GEE Scientific Inc., Kirkland, WA) followed by incubation with NERs containing FITC-Dextran for 45 min at 37°C. After incubation, cells were processed and observed under the fluorescence microscope in the similar manner as described above but Alexa Fluor® 594 goat anti-mouse IgG (Invitrogen, Grand Island, NY) and DAPI were used for staining actin and nucleus of cells, respectively.

### Rho-Kinase Activity Inhibition Assay

For Rho-kinase (ROCK) activity assay, rat PSMCs were cultured as discussed above in a 24-well plate. Cells were divided into 3 groups to receive the following treatments: (i) no treatment, (ii) plain fasudil (45  $\mu\text{M}$ ) and (iii) NERs containing 45  $\mu\text{M}$  fasudil. Cells were activated with lysophosphatidic acid (LPA, 0.5  $\mu\text{g}/\text{ml}$ ) for 2 h prior to treatment for 4 h. Direct measurement of the inhibition of ROCK activity by the fasudil was performed using a Rho-associated protein kinase activity EIA kit (EMD Millipore Corporation, Billerica, MA) according to the manufacturer's protocol. Briefly, cells were lysed, diluted with assay buffer and added to recombinant myosin phosphatase target subunit-1 (rMYPT1) pre-coated wells for 30 min. After this, horseradish peroxidase (HRP) conjugated primary and secondary detection antibodies for MYPT1 were added consecutively followed by 1 h incubation. The amount of phosphorylated substrate was measured by addition of a chromogenic substrate, tetramethylbenzidine (TMB). TMB converts the colorless solution into a blue solution which turns yellow upon addition of the stop solution. The relative amount of ROCK activity in the sample was determined by recording

the absorbance at 450 nm. Cells treated with saline was used as a control and considered as zero percent inhibition for ROCK activity.

### In Vivo Drug Absorption Studies

Drug absorption studies of plain fasudil and fasudil-loaded NERs were conducted in adult male SD rats (250–300 gms) as described previously (18). Animals were divided into 4 groups ( $n=3-4$ ) and anesthetized by giving a cocktail of ketamine and xylazine (90+10 mg/kg) intramuscularly prior to receiving the following treatments: plain fasudil via (i) intravenous (IV) and (ii) intratracheal (IT) routes at a dose of 6 mg/kg and, NERs (suspended in PBS 1X, pH 7.4) equivalent to 6 mg/kg fasudil via (iii) IV and (iv) IT routes. IV dose was administered via the penile vein and IT administration was performed using a PennCentury® Microsprayer for rats. Blood samples were collected into citrated microcentrifuge tubes via tail-vein milking method at different time points for 24 h. The plasma was separated by centrifuging the blood at 5,000 rpm for 5 min and stored at  $-20^\circ\text{C}$  until further analysis.

The concentration of fasudil in plasma samples was determined according to a previously published HPLC method with slight modifications (18). All plasma samples were first deproteinized using an equal volume of acetonitrile and filtered through 0.45  $\mu\text{m}$  filters prior to processing by a Varian HPLC equipped with an autosampler (Varian Prostar 320, Walnut Creek, CA). Mobile phase was an isocratic solvent system comprised of 60% phosphate buffer (0.02 M, pH 7.4) and 40% acetonitrile with a set flow rate of 1 ml/min. 100  $\mu\text{l}$  of clear sample was injected into a C18 column (Inertsil 4  $\mu$  ODS-3, 4.6 $\times$ 250 mm, GL Sciences, Inc., CA, USA) and fasudil was detected by an UV detector at 225 nm. All quantifications were based on a freshly prepared standard curve of plain fasudil in plasma where the elution time was 8.22 min.

All animal studies were performed in accordance with NIH Guidelines for the care and use of Laboratory Animals under a protocol approved by TTUHSC Animal Care and Use Committee (AM-10012).

### Safety Studies

The *in-vitro* safety of the NERs was evaluated by measuring cytotoxicity using an MTT assay in two different cell lines (18). Briefly, rat PASM or human airway epithelial (Calu-3) cells were seeded in a 96-well plate at a density of  $5 \times 10^4$  cells/well and left overnight for adherence. Next day, the cells were incubated with (i) saline (negative control), (ii) 0.1% sodium dodecyl sulfate (SDS, positive control), (iii) plain fasudil (100  $\mu\text{M}$ ) and (iv) NERs (equivalent to 100  $\mu\text{M}$  fasudil) for a period 24 h. The cells were then washed with saline and incubated with 100  $\mu\text{l}$  MTT (0.5 mg/ml in sterile PBS) for

4 h. Subsequently, the formazan crystals were solubilized in dimethyl sulfoxide with moderate shaking on a plate shaker for 1 h. The absorbance was read on a SynergyMX microplate reader (Biotek, Winooski, VT) at 570 nm. The cell viability was calculated using the following equation:  $Percent\ Cell\ viability = (OD_{sample} - OD_{blank}) / (OD_{control} - OD_{blank}) \times 100$ ; OD is density at 570 nm, sample is test compound, control is saline treatment and blank is no treatment.

The *in-vivo* safety of the formulations was assessed by measuring injury markers in BALF according to our published protocols (20). Male SD rats were anesthetized and divided into three groups ( $n=4$ ) to receive following treatments via the intratracheal route: (i) saline (negative control), (ii) NERs (equivalent to 6 mg/kg fasudil), (iii) 0.1% SDS (positive control). After 12 h of administration, individual weight of animals was recorded followed by surgical removal and weighing of lungs which were reported as g/100 g body weight. The BALF was collected and total protein concentration (mg/ml) was assessed by a Bradford assay. The levels of lung injury markers, lactate dehydrogenase (LDH) and alkaline phosphatase (ALP), in BAL fluid were determined using commercial kits (Pointe Scientific, Canton, MI) and reported as IU/L.

### Data Analysis and Statistics

The data are presented as mean  $\pm$  SD and were analyzed by one-way ANOVA followed by Tukey post-hoc analysis using GraphPad Prism 5.0 software (GraphPad Software, San Diego, CA).  $p$  value  $\leq 0.05$  was considered as statistically significant. For pharmacokinetic analysis, standard non-compartmental analysis (WinNonlin®, Pharsight Corp., Cary, NC) was performed to calculate the area under the plasma concentration-time curve from zero to infinity ( $AUC_{0 \rightarrow \infty}$ ), maximum plasma concentration ( $C_{max}$ ), and elimination half-life ( $t_{1/2}$ ).

## RESULTS AND DISCUSSION

In the present investigation, we sought to develop and explore the potential of NERs for intratracheal delivery of an anti-PAH drug, fasudil. Thus we have performed a series of *in-vitro* and *in-vivo* studies to optimize drug loading and stability of fasudil encapsulated NERs and finally evaluated the safety and pharmacokinetics of a selected formulation.

### Preparation of Resealed Erythrocytes

To prepare cells with surface pores, we incubated erythrocytes (Fig. 2a) in hypotonic solutions of varying strengths. By controlling the osmolarity, cells with surface pores between 10 and 500 nm can be prepared. When cells were incubated in

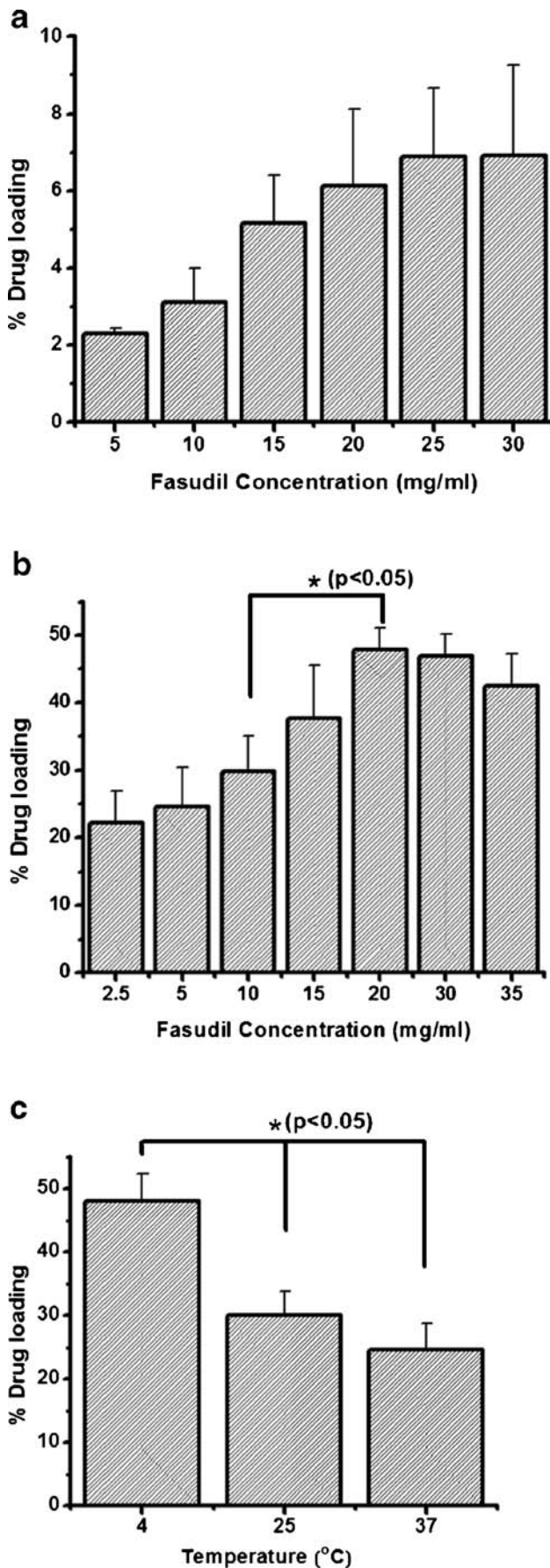
30 mOsm solution, we obtained cell ghosts completely devoid of hemoglobin and intracellular organelles; and hemoglobin depleted cells had numerous pores on the surface (Fig. 2b). The pores on ghost cell membranes were then closed by incubating in hypertonic solution (PBS 10X) at 37°C that resulted in spherical ghost cells. After optimization of preparation parameters, we examined the morphological features of resealed ghosts under a microscope. Hypertonic solution mediated resealing was efficient in retaining spherical morphology of the erythrocytes (Fig. 2c). To assess the drug loading capability of erythrocytes, we encapsulated FITC-dextran into erythrocytes and examined the erythrocytes containing FITC-dextran under a fluorescent microscope. As shown in Fig. 2d, much of the erythrocytic vesicle was filled with FITC-dextran, suggesting that drugs with similar physical property can be encapsulated into erythrocytes.

### Optimization of Drug Loading

First, drug was loaded into resealed erythrocyte ghosts (erythrocytes) (Fig. 1) by simple incubation with drug solution. However, drug loading by this process was minimal. When fasudil was incubated at a concentration of 25 mg/ml with ghosts (Fig. 3a), only  $6.89 \pm 1.78\%$  drug was loaded. Reduced drug loading was perhaps because erythrocyte membrane contained no pores for drug molecule to enter the cells. Alternatively, cell membranes might have lost all transporters during exhaustive hypotonic lysis (10). Further, no increase in drug loading was observed when incubation duration was extended. This data are consistent with the previous assumption that the drug did not move in and out of the cells in the absence of pores (21,22).

But incubation of drug with the ghost cells before resealing resulted in a major increase in drug loading:  $47.81 \pm 3.22\%$  drug was loaded when 20 mg/ml drug solution was incubated with the ghosts (Fig. 3b). Drug loading increased with the increase in concentration from 5 to 20 mg/ml but amount of loading went down when the drug concentration was increased to 30 and 35 mg/ml, which is attributed to saturation of the ghost core. Hence, fasudil solution at a concentration of 20 mg/ml was found to be optimum for maximum drug loading. Drug solution incubated with varying volumes of cell suspension suggests that drug loading was maximal when drug solution-to-ghost cell volume ratio was 1:1 (data not shown). Thus, drug loading was maximal when 500  $\mu$ l fasudil solution (20 mg/ml) was added into 500  $\mu$ l cell suspension.

**Fig. 3** Optimization of drug loading into erythrocyte ghosts: effect of drug concentration on loading after resealing (a), and before resealing (b); effect of temperature on drug loading (c). Data represent mean  $\pm$  standard deviation ( $n=6$ ).



Temperature is an important parameter that influences drug loading into erythrocyte ghosts. So to maximize the entrapment efficiency, drug loading was performed at three different temperatures (4, 25 and 37°C). In consistent with previous studies, drug loading at 4°C was significantly higher compared to that performed at 25°C and 37°C (Fig. 3c). Earlier studies, in fact, demonstrated that cell membrane's pores remain open for a longer time at lower temperature compared to higher temperature (23,24).

### Size Reduction of Erythroosomes and Physicochemical Characterization of Optimized Formulations

We used three different sizing methods to assess their influence on the homogeneity and entrapment efficiency of the formulations. Sizing with sonication produced polydispersed particles (polydispersity index > 0.5) and drastically reduced the entrapment efficiency. But extrusion of ghost cells produced homogeneous particles with a PDI of  $0.105 \pm 1.31$  (Table I). Further, extrusion had minimal effect on entrapment efficiency, suggesting little or no disruption of cells. This is consistent with the flexible structure of erythrocytes that continually travel through narrow capillaries and slits of sinusoids in the physiological system. In fact, structural flexibility is a very important feature of erythrocytes that determines the fate of cells and a slight deviation in terms of shape or rigidity can lead to clearance of cells by macrophages (25). Thus, nanoerythroosomes are expected to be optimal for *in-vivo* efficacy and are likely to avoid clearance by alveolar macrophages.

### Stability of Erythroosomal Formulations

We have evaluated the stability of NERs at varying storage conditions, centrifugal stress, turbulence shock, for hemolytic potential and for influence of nebulization. Compared to storage at room temperature and 37°C, little change in the vesicle size and entrapment efficiency was observed when stored at 4°C. Storage at room temperature resulted in aggregation and leakage of ~60% drug (Table II). Similar to liposomes, NERs are composed chiefly of natural phospholipids and cholesterol (26) and, thus are likely to be stable at 4°C and release the drug for few weeks to as long as several months.

Nebulization breaks larger droplets into smaller ones and delivers the formulations in the form of fine mists. However, the mechanical force produced by nebulization may rupture the formulations and release the drug prematurely. Thus, nebulizability of the formulations were evaluated. No significant differences in vesicle size, polydispersity index and entrapment efficiency were observed before and after nebulization of the NERs (Table III), indicating that nanoerythroosomal integrity was not compromised during

**Table I** The Average Vesicle Size, Polydispersity Indices (PDI) and Entrapment Efficiencies of Nanoerythroosomes Upon Sizing with Various Methods

Method	Size(nm)	PDI	Entrapment efficiency (%)
Bath sonication	286.3 ± 4.67	0.532 ± 0.17	13.65 ± 2.39 <sup>a</sup>
Probe sonication	214.7 ± 8.94	0.712 ± 0.23	17.69 ± 6.78 <sup>a</sup>
Extrusion	154.1 ± 1.31	0.105 ± 0.03	48.76 ± 2.18 <sup>a</sup>

Data represent mean ± standard deviation (n = 6)

<sup>a</sup> Means are significantly different (p < 0.05)

nebulization and the formulations can withstand the force of nebulization.

Centrifugal and turbulence shock stability was determined to assess whether formulations can withstand handling during transportation, dispensing and administration. Entrapment efficiency was essentially unaltered when formulations were centrifuged at 5000 rpm. With the increase in centrifugal force to 15,000 rpm, NERs underwent disruption and released ~50% of the encapsulated drug (Fig. 4a). Similarly, NERs were able to withstand turbulence shock; only 6.79 ± 0.31% drug was released after 20 passes through 27<sup>1/2</sup> gauge needle (Fig. 4b). Both centrifugal and turbulence shock data suggest that NERs based formulations would be resistant to leakage and aggregation.

Upon inhalational delivery, it is possible that some NERs formulations enter the systemic circulation. Thus, we evaluated the potential interaction of NERs with the blood by measuring hemolysis. NERs caused minimal hemolysis even when their concentration was doubled compared with 100% hemolysis caused by water (Fig. 4c). Further, considering that blood volume is much higher than the amount of formulation given, NERs are likely to be safe for inhalational purpose.

### In Vitro Release Studies of NERs Containing Fasudil

The *in vitro* release profiles of fasudil loaded NERs were evaluated in PBS buffer at 37°C. When the release of plain fasudil was evaluated using dialysis cassettes as barriers, ~100% drug

was available in the receiver chamber only after 2 h, suggesting that cassettes were not controlling the passage of drug molecules from donor to receiver chambers. However, only 34.9 ± 1.71% (Fig. 4d) drug was released from fasudil loaded NERs after 2 h and the drug continued to be released for about 48 h. A small amount of drug (11.3 ± 1.32%) was released in 15 min due to burst effect, which can be attributed to surface associated drug or disruption of some cells due to stirring. No degradation in the release media is expected since fasudil remained stable over an extended period of time (~24 weeks) at various storage conditions according to a published report (27). But a slower release may stem from the compact structure of nanoerythroosomal membrane that is composed of natural lipids, cholesterol and surface proteins (7). The *in-vitro* release data suggest that NERs could be used as continuous release carriers for inhalational delivery of fasudil.

### Cellular Uptake of NERs

We expect that NERs containing fasudil would cross the air-blood barrier and produce therapeutic effects in smooth muscle cells by inhibiting ROCK and thus reduce mean pulmonary arterial pressure. NERs (red color, TRITC channel) were observed in the cytoplasm of both PASM and PAE cells (green color, FITC channel) (Fig. 5a and b), suggesting that formulations were taken up by vascular cells that can subsequently produce therapeutic effect. However, further studies using *ex-vivo* lung or double co-culture would perhaps shed light into the mechanism by which NERs moves from respiratory epithelial side to the vascular side.

We have also evaluated the uptake of NERs by alveolar macrophages, because these cells are expected to engulf and remove the particles from the lungs (28). We and others have shown that macrophages could not recognize particles with <250 nm size and thus let the particles escape lung's clearance mechanism (18,29). True to this observation, little or no NERs (green color, FITC channel) were taken up by macrophages (red color of actin, TRITC channel) (Fig. 5c, suggesting that the respiratory clearance mechanism could not

**Table II** Stability Profiles of Nanoerythroosomes Containing Fasudil for 21 days at Three Different Storage Conditions: 4°C, 25°C and 37°C

Days	Storage stability of nanoerythroosomes					
	4°C		25°C		37°C	
	Size (nm)	Entrapment efficiency (%)	Size (nm)	Entrapment efficiency (%)	Size (nm)	Entrapment efficiency (%)
0	154.1 ± 1.31	48.76 ± 2.18	154.1 ± 1.31	48.76 ± 2.18	154.1 ± 1.31	48.76 ± 2.18
7	154.1 ± 1.31	46.32 ± 4.56	179.3 ± 2.31	43.61 ± 3.31	193.7 ± 3.66	37.86 ± 4.39
14	156.2 ± 1.78	41.78 ± 3.11	188.7 ± 3.99	37.66 ± 3.92	204.6 ± 2.98	29.88 ± 3.11
21	189.8 ± 1.43	39.23 ± 2.66	194.7 ± 3.21	32.47 ± 2.18	217.8 ± 4.36	24.61 ± 4.17

Data represent mean ± standard deviation (n = 3)



**Table III** Changes in Vesicle Size, Homogeneity and Entrapment Efficiency Before and After Nebulization

Nebulization	Size (nm)	PDI	Entrapment efficiency (%)
Before	154.31 ± 1.31	0.105 ± 0.03	48.76 ± 2.18
After	156.24 ± 1.97	0.173 ± 0.09	48.39 ± 1.84

Data represent mean ± standard deviation (n = 3)

remove NERs that can help extend the residence time of the drug in the lung.

**In Vitro Rho-Kinase Activity Inhibition Studies**

The efficacy of the formulations in inhibiting ROCK activity in intact cells was evaluated using an antibody capture ELISA assay. ROCK phosphorylates 20 kDa myosin light chain (MLC20) by inactivating myosin phosphatase through phosphorylation of MYPT1 at threonine residue 696 (30), which is detected as a function of ROCK activity in this assay. Rat PASM cells were exposed to LPA to increase ROCK activity (31), which was then treated with either plain fasudil or NERs containing fasudil. Intracellular ROCK levels went down upon exposure to plain fasudil (65.57 ± 7.89%) and NERs containing fasudil (53.39 ± 8.99%) compared with cells that received no treatment (Fig. 6). However, the formulations showed reduced inhibition compared to that produced by plain drug. The reduced ROCK inhibition can be explained by controlled release property of the formulation, which restricted the amount of drug available over the 4-hours treatment period. Since the vasodilatory action of fasudil is mediated by inhibiting ROCK signaling pathway, we anticipate that formulation would be effective in ameliorating the symptoms of PAH. However, more detailed mechanistic studies should provide further information regarding downstream molecules of ROCK signaling pathway.

**In Vivo Drug Absorption Studies of Fasudil Loaded NERs**

The pulmonary absorption of the optimized formulations was studied in adult male SD rats, and compared with the pulmonary and intravenous absorption of plain drug, respectively (Fig. 7, Table IV). NERs extended the half-life of fasudil by

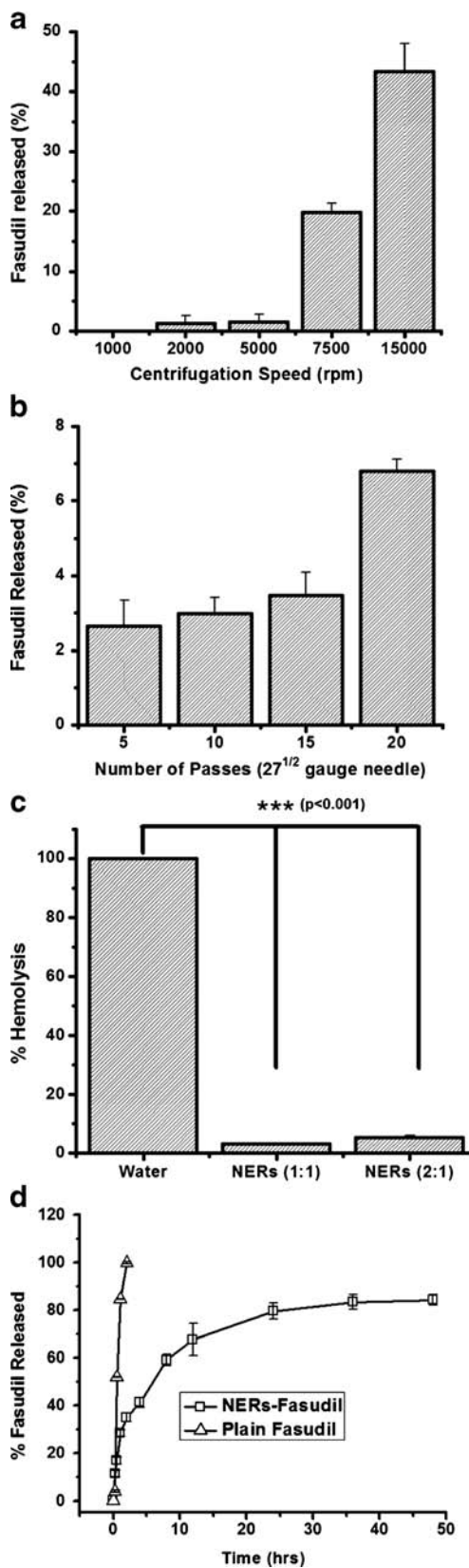
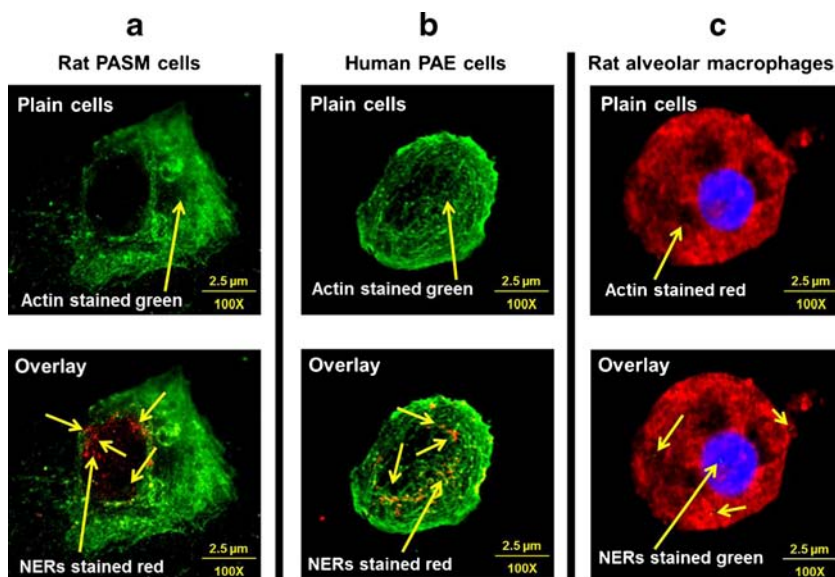


**Fig. 4** In-vitro stability and release profiles of nanoerythrosmes: effect of centrifugation speed (a), turbulence shock (b) (formulation was passed repeatedly through 27<sup>1/2</sup> gauge needle followed by analysis of drug leakage) on the stability of the formulation; the extent of hemolysis upon incubation of formulation in whole blood (c); in-vitro release profiles of plain fasudil and fasudil loaded formulations in PBS (pH 7.4) at 37°C (d). Data represent mean ± standard deviation (n = 3).

~6-8-fold compared with plain fasudil administered via either IV or IT route. However, C<sub>max</sub> did not go up much after IT

**Fig. 5** Uptake of nanoerythroosomes stained with CellMask dye (red) by rat pulmonary arterial smooth muscle cells (a), human pulmonary arterial endothelial cells (b), and uptake of FITC-Dextran (green) loaded nanoerythroosomes by rat alveolar macrophages (c). In case of rat PASM (a) and human PAE (b) cells, cytoskeleton was stained green but in case of rat alveolar macrophages (c), cytoskeleton was stained red.



administration of NERs perhaps because of enhanced retention of fasudil encapsulated in NERs. Plain fasudil was not detectable after 6 h but fasudil in NERs was available in the circulation even after 24 h (Fig. 7). The limit of detection in the HPLC method used was 0.06 μg/ml that was calculated based on the lowest concentration of fasudil providing a signal-to-noise ratio of three (32). The extended circulation time of NERs containing fasudil may stem from the fact that NERs are resistant to enzymatic degradation in the respiratory fluid and act as a drug reservoir in the lung (33). Based on the reported IC<sub>50</sub> of fasudil against Rho-kinase (1.9–3.7 μM) (34), the plasma concentrations of fasudil is likely to maintain the therapeutic concentration for about 24 h. However, the absorption profiles of the formulations do not exactly match the *in-vitro* release profile of the formulation, which may be because of compositional differences between *in-vitro* release media and respiratory fluid. Pulmonary absorption data, however, suggest that NERs

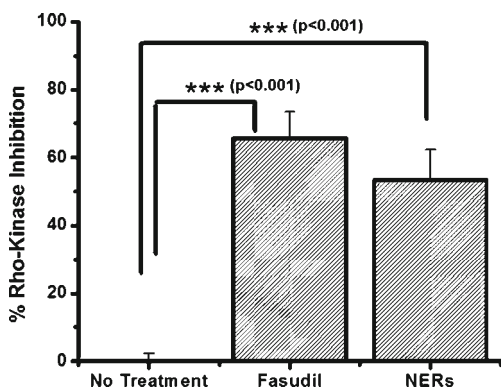


**Fig. 6** Fasudil loaded formulation inhibits Rho-kinase in rat pulmonary arterial smooth muscle cells. Data represent mean ± standard deviation (n=8).

could be an optimal carrier for extended release inhalational formulation.

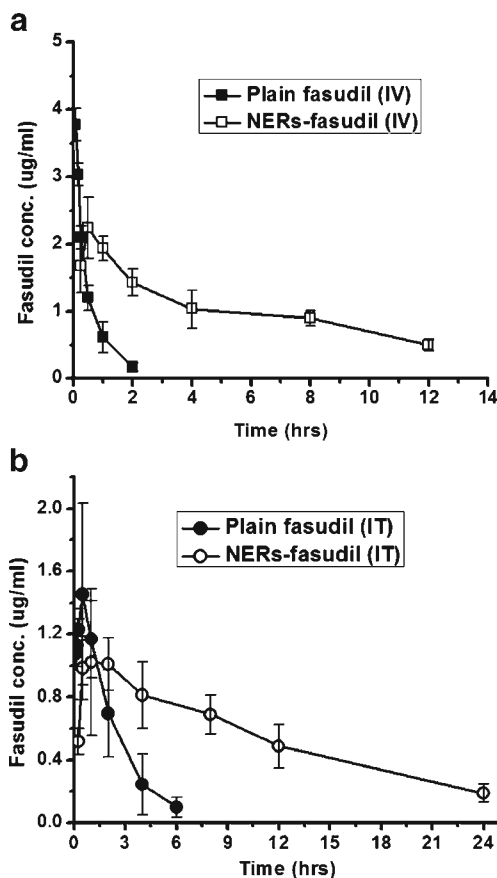


**Fig. 7** *In-vivo* absorption profiles of plain fasudil or nanoerythroosomes containing fasudil administered (a) intravenously (IV) and (b) intratracheally (IT) at a dose of 6 mg/kg. Data represent mean ± standard deviation (n=3).

**Table IV** Pharmacokinetic Parameters of Plain Fasudil and Nanoerythroosomes Containing Fasudil

Treatment	$C_{\max}$ ( $\mu\text{g/ml}$ )	$t_{1/2}$ (hrs)	$AUC_{0 \rightarrow \infty}$ ( $\mu\text{g/ml} \cdot \text{hr}$ )
Fasudil IV	$3.78 \pm 0.23$	$0.53 \pm 0.05$	$27.64 \pm 3.91^a$
Fasudil IT	$1.45 \pm 0.58$	$1.55 \pm 0.08$	$21.72 \pm 4.08^a$
NERs IV	$2.23 \pm 0.45$	$4.61 \pm 0.78$	$23.17 \pm 4.29$
NERs IT	$1.03 \pm 0.17$	$9.69 \pm 1.54$	$31.38 \pm 7.94^a$

Data represent mean  $\pm$  standard deviation ( $n=3$ )

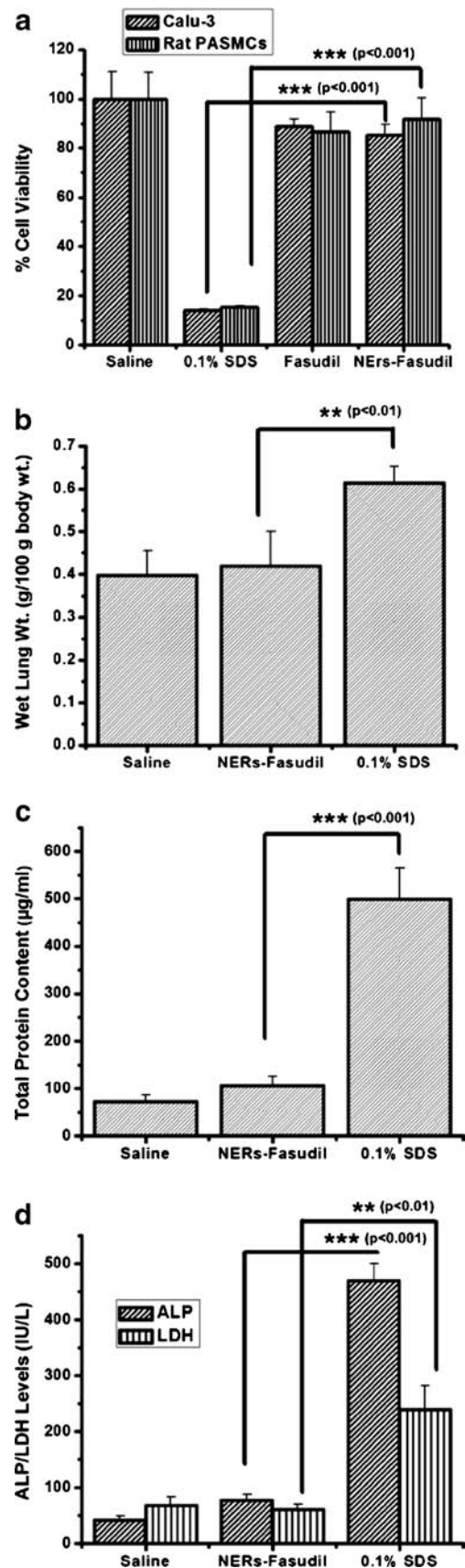
<sup>a</sup> Means are significantly different ( $p < 0.05$ )

### Safety Studies of Formulation

The effect of pure drug and formulations on the viability of two cell lines, Calu-3 and rat PSMCs, was determined using an MTT assay. Cell survival in saline treatment was assumed to be 100% and was used to calculate percentage cell viability in cells treated with drug or formulation (Fig. 8a). The viability of Calu-3 and rat PASM cells was  $85.38 \pm 4.33\%$  and  $91.86 \pm 8.61\%$  respectively, when treated with plain drug or NERs equivalent to  $100 \mu\text{M}$  fasudil for 24 h. But only  $\sim 15\%$  cell viability was observed after SDS treatment. Cell viability data are consistent with the fact that NERs are derived from endogenous materials that are unlikely to cause undesirable side effects.

BALF analysis provides information regarding interaction of inhaled materials with cells lining the respiratory tract. We have measured the total protein content and estimated two injury markers, LDH and ALP, in the BALF collected from rats treated with drug or NERs (35). The wet lung weight of NERs treated rats were slightly higher than that of saline treated ones ( $0.39 \pm 0.05$ ) but significantly smaller than 0.1% SDS treated rats ( $0.61 \pm 0.04$ ), indicating no extensive lung injury due to administration of the formulations (Fig. 8b). A slight difference between the wet lung weights of saline and formulation treated rats may be attributed to edema formation due to intratracheal administration. We found no significant changes in the total protein concentration and levels of either LDH or ALP in NERs treated rats (Fig. 8c and d). But a significant rise in ALP and LDH were observed in case of 0.1% SDS treated rats. While these safety data are encouraging, chronic studies elucidating the pathological

**Fig. 8** Safety of the formulations: The viability of human bronchial epithelial (Calu-3) and rat pulmonary arterial smooth muscle (PASM) cells upon incubation with nanoerythroosomes (a) for 24 h ( $n=12$ ). Effect of the formulation on the wet lung weight (b), total protein content (c), and levels of injury markers (d) in bronchoalveolar lavage (BAL) fluid. Data represent mean  $\pm$  s.d. ( $n=4$ ).



changes after multiple administrations are required to determine the long term safety of the formulations.

## CONCLUSIONS

This study reports the feasibility of nanoerythroosomes as inhalational carriers for a small molecular weight drug, fasudil. Fasudil can be encapsulated into erythrocyte derived carriers with favorable entrapment, *in-vitro* release, and stability profiles. NERs are readily taken up by rat PASM cells, can extend the half-life of fasudil, and appear to be safe for intratracheal delivery. *In-vivo* efficacy studies are underway to evaluate the hemodynamic efficacy of NERs containing fasudil in a rat model of PAH.

## ACKNOWLEDGEMENTS AND DISCLOSURES

The authors acknowledge Drs. Eva Nozik-Grayck and Kurt Stenmark at the University of Colorado, Denver for providing PASM and PAE cell lines. This work was supported in part by an American Recovery and Reinvestment Act Fund, NIH 1R15HL103431 to Dr. Fakhru Ahsan.

## REFERENCES

- Holgado MA, Martin-Banderas L, Alvarez-Fuentes J, Fernandez-Arevalo M, Arias JL. Drug targeting to cancer by nanoparticles surface functionalized with special biomolecules. *Curr Med Chem*. 2012;19:3188–95.
- Allen TM, Cullis PR. Liposomal drug delivery systems: from concept to clinical applications. *Adv Drug Deliv Rev*. 2013;65:36–48.
- Gutiérrez Millán C, Colino Gandarillas CI, Sayalero Marinero ML, Lanao JM. Cell-based drug-delivery platforms. *Ther Deliv*. 2012;3:25–41.
- Yoo JW, Irvine DJ, Discher DE, Mitragotri S. Bio-inspired, bioengineered and biomimetic drug delivery carriers. *Nat Rev Drug Discov*. 2011;10:521–35.
- Patel PD, Dand N, Hirlekar RS, Kadam VJ. Drug loaded erythrocytes: as novel drug delivery system. *Curr Pharm Des*. 2008;14:63–70.
- Magnani M, Pierige F, Rossi L. Erythrocytes as a novel delivery vehicle for biologics: from enzymes to nucleic acid-based therapeutics. *Ther Deliv*. 2012;3:405–14.
- Pouliot R, Saint-Laurent A, Chypre C, Audet R, Vitte-Mony I, Gaudreault RC, *et al*. Spectroscopic characterization of nanoErythroosomes in the absence and presence of conjugated polyethyleneglycols: an FTIR and <sup>31</sup>P-NMR study. *Biochim Biophys Acta*. 2002;1564:317–24.
- Bodemann H, Passow H. Factors controlling the resealing of the membrane of human erythrocyte ghosts after hypotonic hemolysis. *J Membr Biol*. 1972;8:1–26.
- Kwant WO, Seeman P. The erythrocyte ghost is a perfect osmometer. *J Gen Physiol*. 1970;55:208–19.
- Schwoch G, Passow H. Preparation and properties of human erythrocyte ghosts. *Mol Cell Biochem*. 1973;2:197–218.
- Lieber MR, Steck TL. Hemolytic holes in human erythrocyte membrane ghosts. *Methods Enzymol*. 1989;173:356–67.
- Hu CM, Fang RH, Zhang L. Erythrocyte-inspired delivery systems. *Adv Healthc Mater*. 2012;1:537–47.
- Kim SH, Kim EJ, Hou JH, Kim JM, Choi HG, Shim CK, *et al*. Opsonized erythrocyte ghosts for liver-targeted delivery of antisense oligodeoxynucleotides. *Biomaterials*. 2009;30:959–67.
- Mishra PR, Jain NK. Folate conjugated doxorubicin-loaded membrane vesicles for improved cancer therapy. *Drug Deliv*. 2003;10:277–82.
- Agnihotri J, Jain NK. Biodegradable long circulating cellular carrier for antimalarial drug pyrimethamine. *Artif Cells Nanomed Biotechnol*. 2013.
- Lejeune A, Moorjani M, Gicquaud C, Lacroix J, Poyet P, Gaudreault R. Nanoerythroosome, a new derivative of erythrocyte ghost: preparation and antineoplastic potential as drug carrier for daunorubicin. *Anticancer Res*. 1994;14:915–9.
- Schermyly RT, Ghofrani HA, Wilkins MR, Grimminger F. Mechanisms of disease: pulmonary arterial hypertension. *Nat Rev Cardiol*. 2011;8:443–55.
- Gupta V, Gupta N, Shaik IH, Mehvar R, McMurtry IF, Oka M, *et al*. Liposomal fasudil, a rho-kinase inhibitor, for prolonged pulmonary preferential vasodilation in pulmonary arterial hypertension. *J Control Release*. 2013;167:189–99.
- Doberstein SK, Wiegand G, Machesky LM, Pollard TD. Fluorescent erythrocyte ghosts as standards for quantitative flow cytometry. *Cytometry*. 1995;20:14–8.
- Patel B, Gupta V, Ahsan F. PEG-PLGA based large porous particles for pulmonary delivery of a highly soluble drug, low molecular weight heparin. *J Control Release*. 2012;162:310–20.
- Cinti C, Taranta M, Naldi I, Grimaldi S. Newly engineered magnetic erythrocytes for sustained and targeted delivery of anti-cancer therapeutic compounds. *PLoS one*. 2011;6:e17132.
- Zolla L, Lupidi G, Marcheggiani M, Falcioni G, Brunori M. Red blood cells as carriers for delivering of proteins. *Ann Ist Super Sanita*. 1991;27:97–103.
- Sprandel U. Temperature-induced shape transformation of carrier erythrocytes. *Res Exp Med (Berl)*. 1990;190:267–75.
- DeLoach JR, Droleskey RE, Andrews K. Encapsulation by hypotonic dialysis in human erythrocytes: a diffusion or endocytosis process. *Biotechnol Appl Biochem*. 1991;13:72–82.
- Patel VP, Fairbanks G. Spectrin phosphorylation and shape change of human erythrocyte ghosts. *J Cell Biol*. 1981;88:430–40.
- Haran G, Cohen R, Bar LK, Barenholz Y. Transmembrane ammonium sulfate gradients in liposomes produce efficient and stable entrapment of amphipathic weak bases. *Biochim Biophys Acta*. 1993;1151:201–15.
- Ishida T, Takanashi Y, Doi H, Yamamoto I, Kiwada H. Encapsulation of an antispasmodic drug, fasudil, into liposomes, and in vitro stability of the fasudil-loaded liposomes. *Int J Pharm*. 2002;232:59–67.
- Johansson A, Lundborg M, Skold CM, Lundahl J, Tornling G, Eklund A, *et al*. Functional, morphological, and phenotypical differences between rat alveolar and interstitial macrophages. *Am J Respir Cell Mol Biol*. 1997;16:582–8.
- Chono S, Tanino T, Seki T, Morimoto K. Uptake characteristics of liposomes by rat alveolar macrophages: influence of particle size and surface mannose modification. *J Pharm Pharmacol*. 2007;59:75–80.
- Kolozsvári B, Bako E, Becsi B, Kiss A, Czékora A, Toth A, *et al*. Calcineurin regulates endothelial barrier function by interaction with and dephosphorylation of myosin phosphatase. *Cardiovasc Res*. 2012;96:494–503.

31. van Nieuw Amerongen GP, Vermeer MA, van Hinsbergh VW. Role of RhoA and Rho kinase in lysophosphatidic acid-induced endothelial barrier dysfunction. *Arterioscler, Thromb, Vasc Biol.* 2000;20: E127–33.
32. Sanagi MM, Ling SL, Nasir Z, Hermawan D, Ibrahim WA, Abu NA. Comparison of signal-to-noise, blank determination, and linear regression methods for the estimation of detection and quantification limits for volatile organic compounds by gas chromatography. *J AOAC Int.* 2009;92:1833–8.
33. Duncan JE, Hatch GM, Belik J. Susceptibility of exogenous surfactant to phospholipase A2 degradation. *Can J Physiol Pharmacol.* 1996;74:957–63.
34. Masumoto A, Mohri M, Shimokawa H, Urakami L, Usui M, Takeshita A. Suppression of coronary artery spasm by the Rho-kinase inhibitor fasudil in patients with vasospastic angina. *Circulation.* 2002;105:1545–7.
35. Bhargava M, Wendt CH. Biomarkers in acute lung injury. *Transl Res.* 2012;159:205–17.